

[Article]

www.whxb.pku.edu.cn

Ni的化学态对甲烷部分氧化反应机理的影响: 能学分析

夏文生* 常刚 侯玉慧 翁维正 万惠霖*

(固体表面物理化学国家重点实验室, 醇醚酯清洁化工生产国家工程实验室, 福建省理论计算化学重点实验室, 厦门大学化学化工学院, 福建 厦门 361005)

摘要: 采用键指数归一-平方势(UBI-QEP)法对不同化学态Ni上甲烷部分氧化反应中各可能基元步骤进行了能学计算研究. 结果表明, 反应的速度控制步骤与金属Ni的化学态有关. 还原态Ni上CO形成的反应速度控制步骤为表面上CH₃与O物种间的缔合, 而带部分正电荷的Ni上CO形成的反应速度控制步骤则为甲烷氧助解离形成表面CH₃O物种. 还原态和带部分正电荷的Ni中心在表面上共存时, 反应的速度控制步骤将取决于表面CH₃形成与表面CH₃、O物种缔合两反应间的竞争, 其竞争的强弱涉及Ni的化学态. 此外, 反应活性中心向正电荷的Ni转化时, 会导致表面C和O及H和H物种缔合的活化能显著降低, 有利于CO、H₂的形成, 而表面CH₃物种解离则变得不容易, 表面积炭受到明显的抑制.

关键词: 甲烷部分氧化; 镍; 化学态; 速度控制步骤; 机理; 能量学

中图分类号: O641

Influence of Ni Chemical States on the Partial Oxidation Mechanism of Methane: An Energetics Analysis

XIA Wen-Sheng* CHANG Gang HOU Yu-Hui WENG Wei-Zheng WAN Hui-Lin*

(State Key Laboratory of Physical Chemistry for Solid State Surfaces, National Engineering Laboratory for Green Chemical Productions of Alcohols-Ethers-Esters, Fujian Province Key Laboratory of Theoretical and Computational Chemistry, College of Chemistry and Chemical Engineering, Xiamen University, Xiamen 361005, Fujian Province, P. R. China)

Abstract: An energetics analysis of the possible elementary steps involved in the partial oxidation of methane (POM) over different chemical states of Ni was carried out using the unity bond index-quadratic exponential potential (UBI-QEP) method. The results show that the rate determining step for the partial oxidation mechanism of methane is related to the chemical state of the Ni. Over reduced Ni the rate determining step for CO formation is the association of surface CH₃ species with surface O species. Over a partial positive charged Ni surface the rate determining step is that methane dissociates into the CH₃O species with the assistance of oxygen. Over the reduced and partial positive charged Ni sites in coexistence, however, the rate determining step depends on the competition between the formation of surface CH₃ species and the recombination of surface CH₃ species with surface O species. This competition is related to the chemical states of the Ni sites. If the partial positive charged Ni sites are predominant on the surface, the recombination of surface C species with surface O species and the recombination of surface H atom species favor CO and H₂ formation because of decreasing barriers. The surface CH₃ species does not dissociate easily and surface carbon deposition is significantly inhibited.

Key Words: Partial oxidation of methane; Nickel; Chemical state; Rate determining step; Mechanism; Energetics

Received: April 1, 2011; Revised: April 11, 2011; Published on Web: May 6, 2011.

*Corresponding authors. XIA Wen-Sheng, Email: wsxia@xmu.edu.cn; Tel: +86-592-3658107. WAN Hui-Lin, Email: hlwan@xmu.edu.cn.

The project was supported by the National Natural Science Foundation of China (21033006, 20923004), Natural Science Foundation of Fujian Province, China (2007J0168), and National Key Basic Research Program of China (973) (2010CB732303).

国家自然科学基金(21033006, 20923004), 福建省自然科学基金(2007J0168)及国家重点基础研究发展规划项目(973) (2010CB732303)资助

© Editorial office of Acta Physico-Chimica Sinica

1 Introduction

Methane is the major component of natural gas which is thought as an alternative to exhausting petroleum resource. As methane is one of the molecules that most stable in chemistry and mostly located in remote areas, its conversion on site to more useful and easily transportable chemicals, for efficient transportation and utilization, has become a great challenge for scientific community. The discovery that methane is oxidized and converted to synthesis gas is thought as an important breakthrough in methane utilization, since synthesis gas (syngas) can be efficiently converted into a variety of value-added products such as alcohols, ethers and so on.¹⁻³ Several reviews on the conversion of methane to syngas have been given recently.⁴⁻⁶ Two major mechanisms^{5,7} on this conversion have been proposed: a direct mechanism wherein CO is the primary product (partial oxidation mechanism) and an indirect mechanism wherein CO₂ is the primary product (combustion-reforming mechanism) (Fig.1). The target product CO could be produced by reacting surface C atoms with adsorbed O atoms,⁸ and then the rate determining step (RDS) was related to CH_x formation. Nevertheless, CH_xO, as a precursor of the CO formation, was also reported in the literature,⁹ and then the RDS was the reaction of adsorbed hydrocarbon species with adsorbed oxygen species on surfaces.¹⁰ Thus there is a debate on the RDS for the partial oxidation mechanism of methane.

Moreover, Ni is known to be a good catalyst of CO methanation in C₁ chemistry, as C—O bond tends to be broken on the Ni surface, and its RDS is the formation of the CH_x species. In contrast, the Ni is also an efficient catalyst in the partial oxidation of methane (POM) into the CO and H₂, where the C—O bond is formed. This seemingly contradictory could be understood with different chemical states of the Ni between two cases. For the CO methanation active sites are found to be the reduced Ni in presence of H₂, whereas for the POM chemical states of the Ni will be varied with the thickness of catalyst bed during reaction in presence of oxygen, and then the interaction of the Ni with surface species, even the determination of the RDS for the partial oxidation of methane will be affected. As reaction mechanisms for the POM have been reported recently to be related with the chemical states of noble metal catalysts

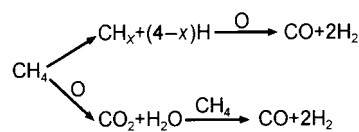


Fig.1 Proposed mechanism for the partial oxidation of methane

by experiments,^{11,12} herein we present an energetics analysis on the partial oxidation mechanism of methane into the CO and H₂ over transition metal Ni to address the issues above.

2 Methods and models

2.1 Methods

We employ the unity bond index-quadratic exponential potential (UBI-QEP) method to obtain reaction energetics (activation barriers and reaction enthalpies). This technique and its previous version, bond order conservation-Morse potential (BOC-MP), have been discussed in detail in two reviews.^{13,14} The assumptions of the UBI-QEP method are: (1) the sum of the bond indices, which are quantitative measures of the bonding interactions, is conserved to unity, (2) the UBI-QEP energy expression is a pair-wise additive function of two-center interactions, (3) the interaction energies between atoms of the adsorbate and the metal surface are spherical having no angular dependence. The UBI-QEP method was developed with the presumption in mind that the active bond (the bond that is breaking or forming) contains at least one atom of the adsorbate that is in contact with the surface. The heats of adsorption are obtained by minimizing the energy subject to the bond index conservation. Activation barriers are extrapolations from the Lennard-Jones intersection of the constrained minimum energy path. The atomic adsorption^{15,16} and gas-phase bond enthalpies¹⁷ as input data are taken from experimental. The predicted heats of adsorption and activation barriers work well and are successfully applied in mechanism study of heterogeneous catalysis reaction widely.^{13,14,18}

2.2 Models

In order to simulate the chemical states of the Ni, we employ assumed thought models, i.e., oxygen pre-adsorbed on Ni(100); Ni(100)-*p*(2×2)O and Ni(100)-*c*(2×2)O (Fig.2), the latter has larger coverage of oxygen than the former on

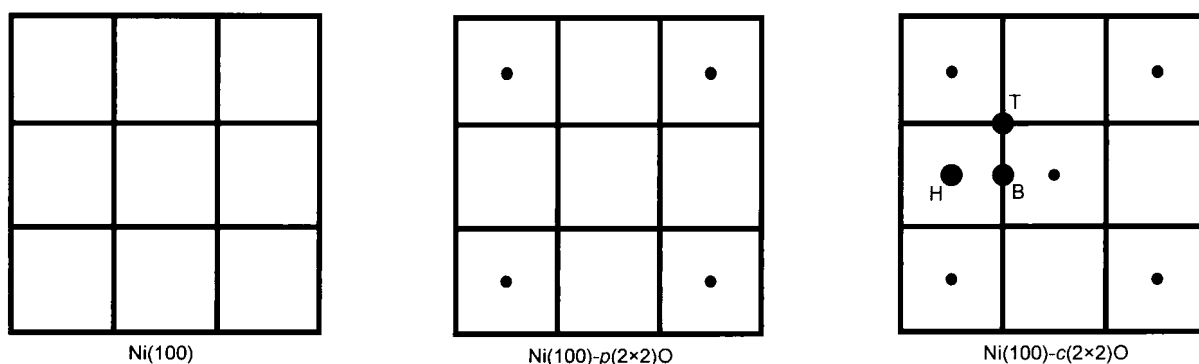


Fig.2 Models of O pre-adsorbed on Ni(100) surfaces for simulation on the chemical states of the catalyst Ni

adsorption site: H, hollow, B, bridge, T, on-top; • pre-adsorbed O, ◦ adsorbate

Table 1 Calculation formula upon adsorption heats (Q_x , $x=A$ or AB) for atom A and molecule AB adsorbed on surface based on the model shown in Fig.2

Adsorption site	Ni(100)- <i>p</i> (2×2)O	Ni(100)- <i>c</i> (2×2)O	h for A	h for AB
T	$Q_x(T)=Q'=hQ_0[1-1/(1+4h/r)^2]$	$Q_x(T)=Q'=hQ_0[1-4/(1+8h/r)^2]$	4/7	1/1
B	$Q_x(B)=2Q'$	$Q_x(B)=2Q'$	3/7	1/2
H	$Q_x(H)=4Q'$	$Q_x(H)=4Q'$	1/4	1/4

x =atom (A) or molecule (AB); $r=Q'_0/Q_x$; Coverage effects have been included into the adsorption heat of oxygen atom (Q'_0). Q' is the interaction energy of x with the single metal site. $Q_x(T)$, $Q_x(B)$, and $Q_x(H)$ are the adsorption heats of x on the on-top, bridge, and hollow sites of the metal Ni surfaces, respectively.

Ni(100) surfaces. As O electronegativity is greater than Ni, the metal Ni atoms nearby will carry more or less positive charges depending on the coverage of oxygen pre-adsorbed on Ni(100) in the assumed thought models. The more the coverage of O pre-adsorbed on Ni, the more the positive charge at Ni sites.

3 Results and discussion

3.1 Calculations on heats of adsorption and activation barriers

Table 1 lists some of the calculation formula upon adsorption heats for species (atom, molecule, etc.) on the modeled surfaces of the partial positive charged Ni. Table 2 shows the predicted heat of adsorption of some relevant species on Ni and their gas-phase active bond enthalpy, with which we can further calculate the activation barrier of the relevant elementary reaction steps (Table 3).

In Table 2, it is found that the heat of adsorption of species on Ni decreases as the positive charge (chemical state) at Ni increases. In Table 3, we list the forward (+) and reversed (−) activation barriers of the relevant elementary reaction steps. C–H bond scission could be either direct or oxygen-assistant, which is obviously related to the chemical states of the metal

Ni. For simulation upon the chemical states of the Ni, the pre-adsorbed oxygen in the assumed thought models is not considered to react with other species on surfaces, and it is just used to adjust or modify the chemical states of the Ni.

3.2 Reactions on reduced Ni

As shown in Table 3, on the reduced Ni (clean Ni(100) surface), comparing reactions No.2 with No.3, we note that CH₄ has significantly lower activation barrier of the direct C–H bond scission than that of O-assistant (61.5 vs 93.3 kJ·mol^{−1}). So, the CH₄ tends to be changed into CH₃+H *via* the direct pyrolysis instead of CH₃O+H or CH₃+OH *via* the O-assistant dissociation. For the C–H bond scission in CH_x ($x=1-3$) species, we find the similar preference of the direct C–H bond cracking to the O-assistant C–H dissociation (cf. reaction Nos.5–6; Nos.8–9; Nos.11–12, in Table 3).

For the species CH₃+H, CH₃ either dissociates into CH₂+H with an activation barrier of 85.4 kJ·mol^{−1} (reaction No.5), or associated with surface O into the CH₃O with an activation barrier of 89.5 kJ·mol^{−1} (the reverse of reaction No.19, denoted as reaction No.19−.) These two channels have very close activation barriers in magnitude, indicating that the two channels are high competitive, and then the formation of the CH₂ (from

Table 2 Gas-phase bond energy, adsorption heat (Q) and coordinated type (η^2 -two contacted atoms of species, μ_2 -two metal atoms) of the relevant species on Ni surfaces

Species	Bond energy/(kJ·mol ^{−1})	Coordinated type	Q /(kJ·mol ^{−1})		
			Ni(100)	Ni(100)- <i>p</i> (2×2)	Ni(100)- <i>c</i> (2×2)
C	—	η^1	753.1	629.7	628.9
H	—	η^1	276.1	174.1	159.8
O	—	η^1	506.3	378.7	377.0
C–H	338.9	η^1	517.6	391.2	388.7
H–CH	422.6	η^1	373.2	257.3	252.7
H–CH ₂	464.4	η^1	198.3	109.2	82.8
H–CH ₃	439.3	$\eta^1\mu_1$	41.8	18.4	0.0
H–CO	75.3	η^1	207.1	116.3	91.2
H ₂ C–O	748.9	$\eta^1\mu_1$	80.3	50.2	36.0
O–CH ₃	376.6	η^1	289.5	184.9	172.0
H–H	431.0	$\eta^2\mu_2$	28.9	9.6	0.0
C–O	1071.1	$\eta^1\mu_1$	123.0	91.2	84.5
O–H	426.8	η^1	274.1	171.5	156.9
O–O	497.9	$\eta^2\mu_2$	77.4	47.7	32.6
O–CO	531.4	$\eta^2\mu_2$	27.6	8.8	0.0
H–OH	426.8	$\eta^1\mu_1$	68.6	39.7	23.0

Table 3 Forward (+) and reversed (–) activation barriers (ΔE^{\ddagger} , ΔE^{\ddagger} , in $\text{kJ}\cdot\text{mol}^{-1}$) for the relevant elementary steps involved into partial oxidation of methane on Ni surfaces

Reaction No.	Reaction	Ni(100)		Ni(100)-p(2×2)O		Ni(100)-c(2×2)O	
		ΔE^{\ddagger}	ΔE^{\ddagger}	ΔE^{\ddagger}	ΔE^{\ddagger}	ΔE^{\ddagger}	ΔE^{\ddagger}
1	$\text{O}_2 \rightarrow \text{O} + \text{O}$	0.0	437.2	0.0	211.7	0.0	223.8
2	$\text{CH}_4 \rightarrow \text{CH}_3 + \text{H}$	61.5	53.1	174.5	0.0	196.6	0.0
3	$\text{CH}_4 + \text{O} \rightarrow \text{CH}_3 + \text{OH}$	93.3	48.1	100.8	0.0	107.9	0.0
4	$\text{CH}_4 + \text{O} \rightarrow \text{CH}_2 + \text{OH}$	101.7	13.4	128.9	0.0	149.8	0.0
5	$\text{CH}_3 \rightarrow \text{CH}_2 + \text{H}$	85.4	73.2	142.3	0.0	134.7	0.0
6	$\text{CH}_3 + \text{O} \rightarrow \text{H}_2\text{CO} + \text{H}$	102.9	39.3	31.8	52.7	23.8	44.4
7	$\text{CH}_3 + \text{O} \rightarrow \text{CH}_2 + \text{OH}$	126.8	31.4	100.0	3.3	92.5	4.6
8	$\text{CH}_2 \rightarrow \text{CH} + \text{H}$	90.8	89.1	117.6	2.9	127.2	0.0
9	$\text{CH}_2 + \text{O} \rightarrow \text{HCO} + \text{H}$	113.0	101.7	56.9	96.2	72.4	78.7
10	$\text{CH}_2 + \text{O} \rightarrow \text{CH} + \text{OH}$	149.4	65.7	111.3	42.3	115.9	35.6
11	$\text{CH} \rightarrow \text{C} + \text{H}$	14.6	187.4	31.4	105.0	33.1	94.1
12	$\text{CH} + \text{O} \rightarrow \text{CO} + \text{H}$	74.5	181.6	0.0	227.6	0.0	210.9
13	$\text{CH} + \text{O} \rightarrow \text{C} + \text{OH}$	82.4	173.6	36.8	155.6	41.8	149.8
14	$\text{H} + \text{H} \rightarrow \text{H}_2$	115.5	22.6	0.0	90.0	0.0	111.3
15	$\text{C} + \text{O} \rightarrow \text{CO}$	184.1	118.8	41.0	195.4	43.1	192.9
16	$\text{CO} + \text{O} \rightarrow \text{CO}_2$	84.5	14.2	1.7	72.0	0.0	69.9
17	$\text{CO} + \text{O} \rightarrow \text{C} + \text{O}_2$	372.0	0.0	366.1	0.0	373.2	0.0
18	$\text{CO}_2 + \text{C} \rightarrow 2\text{CO}$	10.9	15.9	0.0	46.4	0.0	79.9
19	$\text{CH}_3\text{O} \rightarrow \text{CH}_2 + \text{O}$	52.3	89.5	79.1	5.4	88.7	0.0
20	$\text{CH}_3\text{O} \rightarrow \text{H}_2\text{CO} + \text{H}$	43.5	18.8	52.7	0.0	68.6	0.0
21	$\text{H}_2\text{CO} \rightarrow \text{CH}_2 + \text{O}$	82.4	132.6	163.2	0.0	155.2	0.0
22	$\text{H}_2\text{CO} \rightarrow \text{HCO} + \text{H}$	39.7	78.7	123.8	0.0	149.0	0.0
23	$\text{HCO} \rightarrow \text{CH} + \text{O}$	123.4	132.6	173.2	19.2	162.3	29.3
24	$\text{HCO} \rightarrow \text{CO} + \text{H}$	0.0	116.3	0.0	73.6	0.0	77.8
25	$\text{CH}_4 + \text{H} \rightarrow \text{CH}_3 + \text{H}_2$	74.5	66.1	0.0	139.7	0.0	256.5
26	$\text{CH}_3 + \text{H} \rightarrow \text{CH}_2 + \text{H}_2$	3.3	59.0	0.0	80.8	0.0	55.2
27	$\text{CH}_2 + \text{H} \rightarrow \text{CH} + \text{H}_2$	0.0	133.1	0.0	265.7	0.0	402.5
28	$\text{CH} + \text{H} \rightarrow \text{C} + \text{H}_2$	49.8	130.1	0.0	166.1	0.0	172.8
29	$\text{CH}_3\text{O} + \text{H} \rightarrow \text{H}_2\text{CO} + \text{H}_2$	129.7	11.7	24.7	64.9	20.1	62.8
30	$\text{H}_2\text{CO} + \text{H} \rightarrow \text{HCO} + \text{H}_2$	58.2	4.2	35.1	3.8	37.2	0.0
31	$\text{HCO} + \text{H} \rightarrow \text{CO} + \text{H}_2$	47.3	71.1	0.0	166.1	0.0	189.1
32	$\text{H} + \text{O} \rightarrow \text{OH}$	130.1	48.5	36.8	82.4	32.6	79.5
33	$\text{CH}_3\text{O} + \text{OH} \rightarrow \text{H}_2\text{CO} + \text{H}_2\text{O}$	74.5	66.1	0.0	139.7	0.0	256.5
34	$\text{H}_2\text{CO} + \text{OH} \rightarrow \text{HCO} + \text{H}_2\text{O}$	3.3	59.0	0.0	68.2	0.0	55.2
35	$\text{HCO} + \text{OH} \rightarrow \text{CO} + \text{H}_2\text{O}$	0.0	133.1	0.0	265.7	0.0	402.5
36	$\text{CH}_3\text{O} + \text{H} \rightarrow \text{CH}_2 + \text{OH}$	92.0	49.0	59.0	31.0	62.3	20.5
37	$\text{H}_2\text{CO} + \text{H} \rightarrow \text{CH}_2 + \text{OH}$	95.0	63.2	117.6	0.0	108.4	0.0
38	$\text{HCO} + \text{H} \rightarrow \text{CH} + \text{OH}$	125.9	53.1	113.8	5.4	99.2	12.6

CH_3) and the CH_3O (from $\text{CH}_3 + \text{O}$) can exist in parallel.

The CH_2 species further decomposes into $\text{CH} + \text{H}$ with an activation barrier of $90.8 \text{ kJ}\cdot\text{mol}^{-1}$ (see reaction No.8), and then the CH dehydrogenates further into $\text{C} + \text{H}$, which is easy to happen as the barrier is only of $14.6 \text{ kJ}\cdot\text{mol}^{-1}$ (reaction No.11). However, $\text{C} + \text{O} \rightarrow \text{CO}$ has a large barrier of $184.1 \text{ kJ}\cdot\text{mol}^{-1}$ (see reaction No.15), the reaction will stop at the formation of the C, resulting in the carbon deposition on surfaces, and the RDS for the carbon formation from the CH_4 will be $\text{CH}_2 \rightarrow \text{CH} + \text{H}$

with a barrier of $90.8 \text{ kJ}\cdot\text{mol}^{-1}$. This is comparable to the barrier of methane pyrolysis on the Ni reportedly ($98.7 \text{ kJ}\cdot\text{mol}^{-1}$).¹⁹ Another channel coexist with the CH_2 transformation on surfaces, is the transformation of the CH_3O on surfaces. The CH_3O (reaction Nos.20, 22, 24 in Table 3) is easy to dehydrogenate step-wisely until the formation of CO, the relevant barrier is $43.5, 39.7, 0.0 \text{ kJ}\cdot\text{mol}^{-1}$, respectively. Thus the RDS from CH_4 to CO should be $\text{CH}_3 + \text{O} \rightarrow \text{CH}_3\text{O}$ ($\Delta E^{\ddagger} = 89.5 \text{ kJ}\cdot\text{mol}^{-1}$), which is in accord with the pulse-MS study on the partial oxidation

mechanism of methane,¹⁰ and close to the reported barrier (77.0 kJ·mol⁻¹).⁴

As the heat of adsorption of CO on Ni(100) is 123.0 kJ·mol⁻¹ (Table 2), if the remaining time of the CO on Ni is long enough, Boudart reaction CO+CO→C+CO₂ (reaction No.18—: Δ*E*^{*}=15.9 kJ·mol⁻¹; Δ*H*=5.0 kJ·mol⁻¹), will result in some carbon deposition on the Ni surfaces. Combining with the above analysis on the direct decomposition of the species CH_x into the C, we think that the carbon deposition is easily happened on Ni as observed experimentally.⁶

It is notable in Table 3, several reactions CH_x (x=1–4)+H→CH_{x-1}+H₂ (reaction Nos.25–28) and CH_xO(x=1, 2)+H→CH_{x-1}O+H₂ (reaction Nos.30–31), have not so large barrier, indicating that the CH_x or CH_xO could have new transformation channels if the H atom species on surfaces is not so diffusive. These channels to the H₂ formation give far smaller barriers than H+H→H₂ (reaction No.14).

Therefore, for the POM reaction over the reduced Ni, CO formation comes from the dehydrogenation of CH_xO instead of the recombination of C with O, and the RDS for the CO formation is CH_x+O→CH_xO, and the formation and decomposition of the CH_x species is paralleled channel with the formation and transformation of the CH_xO species. This result is not in conflict with the fact that the mechanism upon the surface CH_x species formation not supported by the isotropic effect reportedly,²⁰ and the carbon deposited on Ni is arisen from the paralleled channel upon the CH_x decomposition. The H₂ formation from the channel upon the association of the H atoms themselves should be of low probability if on the reduced Ni, and that from H-assistance dissociation of the CH_x species is more likely.

3.3 Reactions on the partial positive charged Ni surfaces

On the partial positive charged Ni surfaces, simulated with Ni(100)-*p*(2×2)O and Ni(100)-*c*(2×2)O (assumed thought models: oxygen pre-adsorbed on Ni surfaces), the positive charge at the Ni sites for the later is more than that for the former.

As shown in Table 3, on Ni(100)-*p*(2×2)O and Ni(100)-*c*(2×2)O, the direct pyrolysis of the CH₄ has high activation barriers (174.5 and 196.6 kJ·mol⁻¹, reaction No.2), while O-assistance dissociation of CH₄ into CH₃O+H has smaller barriers (100.8 and 107.9 kJ·mol⁻¹, reaction No.3), so the C—H bond scission of methane on the partial positive charged Ni surfaces tends to be oxygen assistant, which is different from that on reduced the Ni surfaces.

Once the CH₃O is formed, it can either dehydrogenate into H₂CO+H with barriers of 52.7 and 68.6 kJ·mol⁻¹ on the two assumed Ni surfaces, or react with the H atom species nearby into CH₃+OH with barriers of 59.0 and 62.3 kJ·mol⁻¹, or into H₂CO+H₂ with barriers of 24.7 and 20.1 kJ·mol⁻¹ (cf. reaction Nos.19–20, 29, 36). H₂CO has large barriers to decompose directly into HCO+H (123.8 and 149.0 kJ·mol⁻¹), and then it can only dissociate with H- or OH-assistance into HCO+H₂/H₂O (cf. reaction Nos.21, 22, 30, 34, 37) provide that the H atom

species is not so diffusive, as the barriers are only 35.1 and 37.2 kJ·mol⁻¹ respectively on the two Ni surfaces with partial positive-charge. HCO, from reaction Nos.23, 24, 31, and 38, is found to decompose into the CO easily. The formed CO becomes not so stable with the increase of the positive charge at the Ni sites, since the CO is easily oxidized into CO₂ (the barriers are 1.7 and 0.0 kJ·mol⁻¹) in contrast to that on the reduced Ni surface (the barrier is 84.5 kJ·mol⁻¹) (reaction No.16), and then the probability of the CO₂ formation is increased, but the CO₂ can react with the surface carbon C species to form the CO easily with no activation barriers (reaction No.18), and the surface carbon C species could be formed from H-assistance dissociation of the CH_x (reaction Nos.25–28). So, CO formation is arisen from the step-wise dehydrogenation of CH_xO species (less than ~71 kJ·mol⁻¹) and the reverse of Boudart reaction (reaction No.18), and the primary product is partially CO₂, the RDS is CH_x+O→CH_xO+H. The carbon deposition on Ni surfaces can be eliminated due to the reverse of Boudart reaction.

Also, the carbon C on surfaces can recombine with O into the CO more easily on the partial positive charged Ni than on the reduced Ni (C+O→CO, Δ*E*^{*}: 184.1 kJ·mol⁻¹ vs ~40 kJ·mol⁻¹), indicating that the carbon formation on the partial positive charged Ni surfaces is quite unfavorable in energy, and there should be much decreased deposition of carbon on surfaces. This result is also supported by the fact that the influence of different rare earth oxide supported Ni on the rate of the carbon deposition was related to oxygen release ability of rare earth oxides as the support.⁶ Generally, the barrier of the CH_x association with O is decreased (reaction Nos.15, 19–, 21–, 23–), and the CH_x dissociation barrier is generally increased (reaction Nos.2, 5, 8, 11), if the positive charge at the Ni sites increases.

The H atom species associates with the O atom species into OH with lower barriers (36.8 and 32.6 kJ·mol⁻¹) on the partial positive charged Ni surfaces than that on the reduced Ni surface (reaction No.32), and the OH species can make the CH_xO dehydrogenation easy due to thermodynamic driving by H₂O formation (reaction Nos.33, 34).

The H₂ formation could be arisen from H-assistance dissociation of the CH_x/CH_xO as discussed above, or from the recombination of the H atoms species themselves, as H+H→H₂ reaction occurs with no activation barrier on the partial positive charged Ni surfaces, significantly different from that on the reduced Ni surface.

Therefore, on the partial positive charged Ni surfaces, the CO formation is arisen from three channels: the dehydrogenation of the CH_xO, the recombination of C with O and the reverse of Boudart reaction, and then the carbon deposition is much decreased. The RDS is CH_x+O→CH_xO+H. The reaction intermediate CH_x decomposition and its association with O are much relevant to the chemical states of the Ni.

3.4 Reactions on the reduced and partial positive charged Ni sites in coexistence

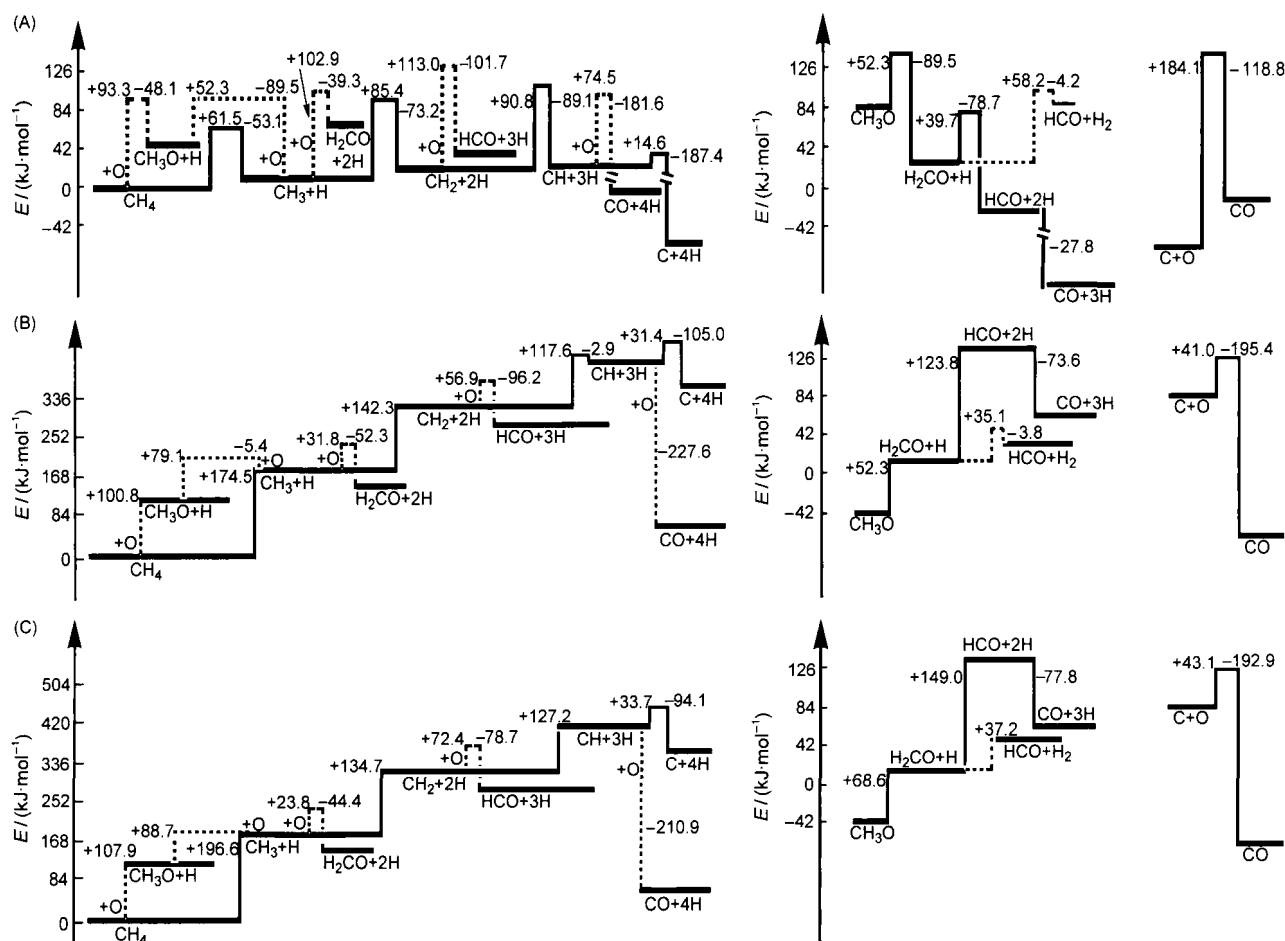


Fig.3 Diagrams of predicted activation barriers of some important elementary steps involved into partial oxidation of methane on different surfaces by UBI-QEP method

(A) Ni(100), (B) Ni(100-*p*(2×2)O), (C) Ni(100)-*c*(2×2)O; The positive and negative data in the diagram are the forward and reversed activation barrier of elementary steps, respectively

As a matter of fact, metal surface is oxidized more or less in presence of oxygen under the POM reaction conditions, and then it is possible to be coexistent for the reduced and partial positive charged Ni sites on the surfaces, which is related to the thickness of catalyst bed and the interaction between metal and supports, and etc. Fig.3 is a simplified schematic of energetics for some key steps upon the partial oxidation mechanism of methane on the different chemical states of the Ni. As shown in Fig.3, on the reduced Ni, the CH₃ species is relatively easy to form (activation barrier: 61.5 kJ·mol⁻¹), and the CH₃ recombines with O into the CH₃O, which dehydrogenate step-wisely until the CO is formed, the largest barrier in the series of steps is 89.5 kJ·mol⁻¹, and the RDS is CH₃+O→CH₃O, however, if the partial positive charged Ni is coexistent and participates in the reaction, the formed CH₃ species will rapidly react with O into the CH₃O, and then dehydrogenate until the CO formation, the largest barrier in those processes is 61.5 kJ·mol⁻¹, and the RDS is the CH₃ formation from the C—H bond scission of methane. Thus, the activation barrier of the RDS on the reduced Ni is 89.5 kJ·mol⁻¹, and on the reduced and partial positive charged Ni in coexistence is 61.5 kJ·mol⁻¹, which is in good agreement with the reported values (77.0 kJ·mol⁻¹,⁴ 64.9

kJ·mol⁻¹). So the RDS for the partial oxidation mechanism of methane is much related to the chemical states of the metal Ni, and then the activation barriers of reaction are also affected by the chemical states of the Ni.

Honestly, the reaction rate is related to the activation barriers (exponential factors) and entropies (pre-exponential factors), but it is still significant for the above energetics analysis, especially for the comparison of reactions on the different chemical states of metal surfaces, as those comparisons are made on the basis of the similar entropies in most cases.

4 Conclusions

On reduced Ni, the pyrolysis of CH₃ from CH₄ and association of CH₃ with O (CH₃+O→CH₃O) are competitive channels in parallel, and the RDS for the CO formation is CH₃+O→CH₃O. The CO comes from the step-wise dehydrogenation of the CH₃O, and the carbon from the CH₄ pyrolysis can deposit on the surface. The H₂ comes quite likely from the H-assisted dissociation of the CH₄ and CH₃O.

On the partial positive charged Ni, the O-assisted dissociation of CH₄ into the CH₃O is significantly favored over CH₄ pyrolysis energetically, and becomes predominant, and the RDS

is the CH₃O formation from CH₄. The CO comes from three channels: the dehydrogenation of CH₃O, the recombination of C with O, and the reverse of Boudart reaction, and then the carbon deposition on the Ni surfaces can be much decreased. The H₂ comes from three channels: the recombination of the H atoms themselves, the H-assistant dissociation of CH₃, the H-assistant dissociation of the CH₃O.

On the reduced and partial positive charged Ni in coexistence, the RDS depends on the competition between the formation of the CH₃ and the association of CH₃ with O, which is related to the chemical states of the metal Ni. In addition, the CO formation is mainly arisen from the dehydrogenation of CH₃O ($x > 0$).

As the positive charge at the Ni sites increases, the probability of the CH₃ decomposition decreases, but that of association of the CH₃ with O increases.

References

- (1) Trimm, D. L.; Onsan, Z. I. *Catal. Rev. Sci. Eng.* **2001**, *43*, 31.
- (2) Specchia, S.; Negro, G.; Saracco, G.; Specchia, V. *Appl. Catal. B* **2007**, *70*, 525.
- (3) Burke, N. R.; Trimm, D. L. *Catal. Today* **2006**, *117*, 248.
- (4) Enger, B. C.; Lodeng, R.; Holmen, A. *Appl. Catal. A* **2008**, *346*, 1.
- (5) York, A. P. E.; Xiao, T.; Green, M. L. H. *Top. Catal.* **2003**, *22*, 345.
- (6) Choudhary, T. V.; Choudhary, V. R. *Angew. Chem. Int. Edit.* **2008**, *47*, 1828.
- (7) Hu, Y. H.; Ruckenstein, E. *Adv. Catal.* **2004**, *48*, 297.
- (8) Lu, Y.; Xue, J. Z.; Yu, C. C.; Liu, Y.; Shen, S. K. *Appl. Catal. A* **1998**, *174*, 121.
- (9) Xu, J. G.; Froment, G. F. *AICHE J.* **1989**, *35*, 88.
- (10) Tang, S.; Lin, J.; Tan, K. L. *Catal. Lett.* **1998**, *55*, 83.
- (11) Rabe, S.; Nachttegaal, M.; Vogel, F. *Phys. Chem. Chem. Phys.* **2007**, *9*, 1461.
- (12) Liu, Y.; Huang, F. Y.; Li, J. M.; Weng, W. Z.; Luo, C. R.; Wang, M. L.; Xia, W. S.; Huang, C. J.; Wan, H. L. *J. Catal.* **2008**, *256*, 192.
- (13) Shustorovich, E.; Sellers, H. *Surf. Sci. Rept.* **1998**, *31*, 1.
- (14) Shustorovich, E. *Adv. Catal.* **1990**, *37*, 101.
- (15) Rhodin, T. N.; Ertl, G. In *The Nature of the Surface Chemical Bond*; North-Holland Publ.: Amsterdam, 1979; Tables 5.1.
- (16) Brennan, D.; Hayward, D. O.; Trapnell, B. M. W. *Proc. R. Soc. London, Ser. A* **1960**, *256*, 81.
- (17) In *CRC Handbook of Chemistry and Physics*; CRC Press: Boca Raton, Florida, 1984–1985; p F171.
- (18) Xia, W. S.; Sellers, H. *Surf. Sci.* **2003**, *524*, 15.
- (19) Wei, J.; Iglesia, E. *J. Catal.* **2004**, *224*, 370.
- (20) Hu, Y. H.; Ruckenstein, E. *Catal. Lett.* **1999**, *57*, 167.
- (21) Theron, J. N.; Dry, M. E.; Steen, E. V.; Fletcher, J. C. Q. *Stud. Surf. Sci. Catal.* **1997**, *107*, 455.